Dynamic Response Analysis of Rotating Composite-VEM Thin-Walled Beams Incorporating Viscoelastic Materials in the Time Domain

Sungsoo Na*, Jaeyong Park
Corresponding Author, Department of Mechanical Engineering, Korea University, Seoul 136-701, Korea
Chul H. Park
Department of Mechanical Engineering, Pohang University of Science and Technology, Pohang 790-784, Korea
Moon K. Kwak
Department of Mechanical Engineering, Dongguk University, Seoul 100-715, Korea
Jae-Hong Shim
Department of Mechatronics Engineering, Korea Polytechnic University, Siheung City, Keonggi-do 429-793, Korea

This paper addresses the analytical modeling and dynamic response of the advanced composite rotating blade modeled as thin-walled beams and incorporating viscoelastic material. The blade model incorporates non-classical features such as anisotropy, transverse shear, rotary inertia and includes the centrifugal and coriolis force fields. The dual technology including structural tailoring and passive damping technology is implemented in order to enhance the vibrational characteristics of the blade. Whereas structural tailoring methodology uses the directionality properties of advanced composite materials, the passive material technology exploits the damping capabilities of viscoelastic material (VEM) embedded into the host structure. The VEM layer damping treatment is modeled by using the Golla-Hughes-McTavish (GHM) method, which is employed to account for the frequency-dependent characteristics of the VEM. The case of VEM spread over the entire span of the structure is considered. The displayed numerical results provide a comprehensive picture of the synergistic implications of both techniques, namely, the tailoring and damping technology on the dynamic response of a rotating thin-walled beam exposed to external time-dependent excitations.

Key Words: Thin-Walled Composite Beam, Viscoelastic Material, GHM Method, Passive Damping

1. Introduction

The rotating cantilevered composite thin-walled beam structure is the most important structure that can serve as a basic model for a number of constructions used in the aeronautical and space industries, such as airplane wings, helicopter blades, fan blades, robotic manipulator arms and space booms, etc.

For such structures, the development and implementation of adequate methodologies aiming at controlling their free and forced vibration char-

* Corresponding Author,
E-mail : nass@korea.ac.kr
TEL : +82-2-3290-3370; **FAX** : +82-2-926-9290
Corresponding Author, Department of Mechanical Engineering, Korea University, Seoul 136-701, Korea. (Manuscript **Received** August 26, 2005; **Revised** May 11, 2006)

acteristics are likely to contribute to the improvement of their performance and avoidance of the occurrence of resonance and any dynamic instability. An important step toward the rational design of modern rotor blades and propellers consists of the development of analytical models that are capable to accurately predicting their dynamic behaviors.

One of the possible ways towards achieving such goals consists in the implementation of viscoelastic materials (VEM) embedded or spread into the host structure, which increase the energy dissipation due to the characteristics of VEM which minimize vibrations to improve resiliency. For instance, increasing the damping levels in turbo-fan blades is of current interest to both NASA and the Air Force as a means of making commercial and military turbo-fan engines more reliable. Increasing the damping capabilities in the beams or blades will improve the fatigue life, operation range and vibration characteristics and reduce vibration level and aeroelastic instability matter. The appropriate viscoelastic finite element modeling of VEM will be called the GHM (Golla-Hughes-McTavish) method and the system can be analyzed in the time domain. Validation of the method is well defined in earlier monographs. (Lam et al., 1997)

A considered damping material is 3M ISD 112, which offers higher damping (loss) factors than any other available vendor-supplied ones. Although of an evident importance, to the best of author's knowledge, no such studies including vibration and dynamic analysis of rotating composite-VEM thin-walled blade exposed to external loads can be found in the specialized literature. The early works on analyses of sandwich structures with a viscoelastic core were done by Kerwin (1959) and Ross et al. (1959), DiTaranto (1965), and Mead and Markus (1969). They presented the fourth and sixth-order theories for beams and plates to predict damping and handled the cases with arbitrary boundary conditions. The governing equations of flexural vibration of symmetrical sandwich rectangular plate were presented by Mead and Markus (1969). Rao and Nakra (1974) proposed a set of 12^{th}-order partial differential governing equation including bending-extension coupling of unsymmetrical beams and plates with a viscoelastic core were discussed. C. Park et al. (1998) derived a new technique to formulate the finite element model of a sandwich beam by using GHM. C. Park et al. (2005) presented the modeling of a hybrid passive damping system for suppressing the multiple vibration modes of beams, which consists of a constrained layer damping and a resonant shunt circuit.

In this paper, a study of free and forced vibration in both the in-plane (lagging) and transverse to the plane of rotation (flapping) of rotating beams is addressed. Moreover, by incorporating the capability referred to as viscoelastic induced damping scheme control of coupled flapping-lagging vibration is carried out.

2. Formulation of the Composite-VEM Thin-Walled Beam

The model of the host structure considered encompasses a number of features such as: (a) transverse shear, (b) anisotropy of constituent materials, (c) rotary inertia, (d) the beam cross-sections feature a symmetric biconvex profile, while VEM layer is assumed to be isotropic material. Its geometric configuration and the typical cross-section along with the associated system of coordinates are presented in Fig. 1. The inertial coordinates XYZ is attached to the center of the hub O, and the origin of the rotating axis xyz is located at the blade root at an offset R_0, which denotes the radius of the hub. The points of the beam cross-sections are identified by the global

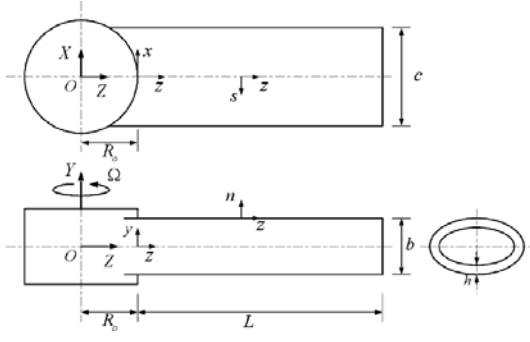

Fig. 1 Rotating blade and coordinate used

coordinates x, y and z, where z is the spanwise coordinate and by a local one, n, s, and z, (see Fig. 1) where n and s denote the thicknesswise coordinate normal to the beam mid-surface and the tangential one along the contour line of the beam cross-section, respectively.

In present study, the rotation takes place in the XZ plane with a constant angular velocity Ω. The equations of rotating thin-walled beams are based upon the following statements (Shim and Na, 2003): i) The original cross-section of the beam is preserved, ii) the transverse shear effects are taken into account, iii) the circumferential stress resultant N_{ss} (i.e., the hoop stress resultant) is negligibly small when compared to the remaining ones, iv) the case of a bi-convex beam cross-section profile is adopted. In accordance with the above assumptions and in order to reduce the 3-D problem to an equivalent 1-D, the components of the displacement vector in the composite host structure are expressed as

$$\begin{aligned} u(x,y,z,t) &= u_0 - y\Theta(z,t) \\ v(x,y,z,t) &= v_0 + x\Theta(z,t) \\ w(x,y,z,t) &= w_0(z,t) + \theta_x(z,t)\left[y(s) - n\frac{dx}{ds}\right] \\ &\quad + \theta_y(z,t)\left[x(s) + n\frac{dy}{ds}\right] \\ &\quad - \Theta'(z,t)\left[F_w(s) + na(s)\right] \end{aligned} \quad \text{(1a, b)}$$

$$\begin{aligned} \theta_x(z,t) &= \gamma_{yz}(z,t) - v_0'(z,t) \\ \theta_y(z,t) &= \gamma_{xz}(z,t) - u_0'(z,t) \end{aligned} \quad \text{(2a, b)}$$

Eqs. (1) and (2) reveal that kinematic variables $u_0(z,t)$, $v_0(z,t)$, $w_0(z,t)$, $\theta_x(x,t)$, $\theta_y(z,t)$, and $\Theta(z,t)$ representing three translations in the x, y, z directions and three rotations about the x, y, z directions, respectively are used to define the displacement components, u, v and w. Furthermore, γ_{yz} and γ_{xz} denote the transverse shear in the planes yz and xz respectively and the primes denote derivatives with respect to the z-coordinate. The primary warping function is expressed as (Shim and Na, 2003)

$$F_w = \int_0^s [r_n(s) - \psi]\, ds \tag{3}$$

where the torsional function ψ and the quantity $r_n(s)$, $a(s)$ are

$$\psi = \frac{\oint_c \frac{r_n(s)}{h(s)} ds}{\int_c \frac{ds}{h(s)}} \tag{4}$$

and

$$r_n(s) = x(s)\frac{dy}{ds} - y(s)\frac{dx}{ds} \tag{5}$$

$$a(s) = -y(s)\frac{dy}{ds} - x(s)\frac{dx}{ds} \tag{6}$$

Figure 2 reveals the geometrical meaning of $a(s)$ and $r_n(s)$ as well. The position vector of a point $M(x,y,z)$ belonging to the deformed structure is

$$\mathbf{R}(x,y,z,t) = (x+u)\mathbf{i} + (y+v)\mathbf{j} + (z+w)\mathbf{k} + \mathbf{R}_0 \tag{7}$$

Recalling that the spin rate was assumed to be constant, with the help of equations expressing the time derivatives of unit vectors, one obtains the velocity and acceleration vectors of a point M under the form

$$\begin{aligned} \dot{\mathbf{R}} &= V_x\mathbf{i} + V_y\mathbf{j} + V_z\mathbf{k} \\ &= (\dot{u} + (R_0+z)\Omega)\mathbf{i} + \dot{v}\mathbf{j} - ((x+u)\Omega)\mathbf{k} \end{aligned} \tag{8}$$

$$\begin{aligned} \ddot{\mathbf{R}} &= a_x\mathbf{i} + a_y\mathbf{j} + a_z\mathbf{k} \\ &= (\ddot{u} - (x+u)\Omega^2)\mathbf{i} + \ddot{v}\mathbf{j} \\ &\quad + (-2\dot{u}\Omega - (R_0+z)\Omega^2)\mathbf{k} \end{aligned} \tag{9}$$

Herein $\eta \equiv z/L$ is the dimensionless spanwise coordinate ($\eta \in [0, 1]$), where L denotes the wing semi-span, c and b denote the local wing chord

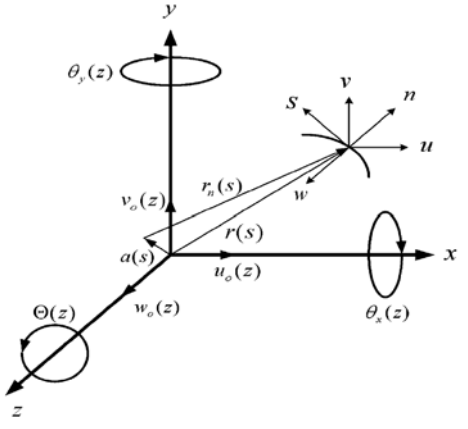

Fig. 2 Displacement field for thin walled beam

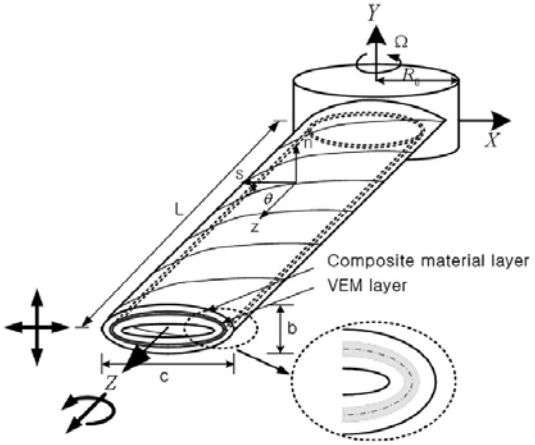

Fig. 3 Typical configuration of composite-VEM-composite thin walled blade

and height, respectively. As result of the considered anisotropy of the structure and consideration of CUS (Circumferentially Unsymmetric Stiffness) manufacturing technique (Oh et al., 2003), an exact decoupling of coupled transverse (flapping)-chorwise (lagging) bending expressed in terms of variables v_0, θ_y, u_0 and θ_x and coupled twist (Θ)-axial (w_0) motion is implemented. For the problem studied herein, the coupled flapping and lagging motions will be considered only. Fig. 3 shows the typical composite-VEM thin walled blade model that is considered in the present analysis.

3. Golla-Hughes-McTavish Representation of VEM

A system which has viscoelastic damping is often modeled as having a complex modulus. However, use of the complex modulus directly in the equation of motion leads to a dynamic model useful only at single-frequency steady-state excitations. The Golla-Hughes-McTavish (GHM) modeling approach (McTavish and Hughes, 1992) provides an alternative method which includes viscoelastic damping effects without the restriction of steady-state motion by providing extra coordinates. GHM model introduces hysteretic damping by adding additional "dissipation coordinates" to the system to achieve a linear non-

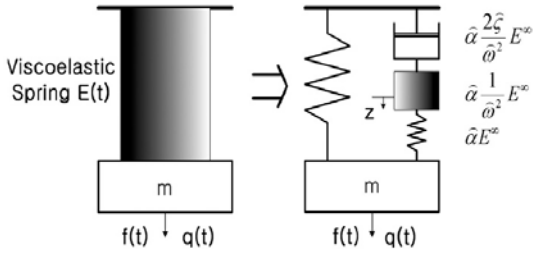

Fig. 4 The "mini-oscillator" mechanical analogy

hysteretic model providing the same damping properties. The dissipation coordinates are used with a standard finite element approach or, as in this work, with assumed modes method. The derivation of the GHM equations starts with the constitutive relation for a one dimensional stress-strain system using the theory of linear viscoelasticity.

$$\sigma(t)=E(t)\,\varepsilon(0)+\int_0^t E(t-\tau)\frac{d}{d\tau}\varepsilon(\tau)\,d\tau \quad (10)$$

It is assumed that the strain, ε is zero for all time less than zero, and $E(t)$ is defined as a material modulus function. The GHM scheme requires the representation of the material modulus function as a series of "mini-oscillator" terms or internal variables. Each mini-oscillator term is a second order rational function involving three positive constants, $\{\hat{\alpha},\hat{\omega},\hat{\zeta}\}_k$. Fig. 4 represents the mechanical analogy of one modulus system for a single degree of freedom. The time domain stress relaxation is modeled by a modulus function in the Laplace domain. This complex modulus can be written in Laplace domain from Eq. (10) as

$$\sigma(s)=sE(s)\,\varepsilon(s) \quad (11)$$

$$E(s)=E^{\infty}(1+h(s)) =E^{\infty}\left(1+\sum_{n=1}^{k}\hat{\alpha}_n\frac{s^2+2\hat{\zeta}_n\hat{\omega}_n s}{s^2+2\hat{\zeta}_n\hat{\omega}_n s+\hat{\omega}}\right) \quad (12)$$

where E^{∞} is the equilibrium value of the modulus, i.e. the final value of the modulus function $E(t)$, and s is the Laplace domain operator. The hatted terms are obtained from the curve fit to the complex modulus data for a particular VEM at a given temperature. Also, the number of expansion terms, k may be modified to represent the high or low frequency dependence of the complex terms.

The expansion of $k(s)$ represents the material modulus as a series of the mini oscillator (second order equation) terms. The both real and imaginary part of Young's modulus for 3M ISD-112 at temperature 25℃ are plotted in Fig. 5. These are compared to the corresponding curve fitted line indicated by solid line using 1~4 mini oscillator terms. The curve fitted line is well defined to represent the true value of Young's modulus in frequency range between $10^2 \sim 10^3$ rad/sec, of which range is interested in the present study. It is noted that the Young's modulus is greater for increasing frequency.

The equation of motion for a single modulus model with n expansion terms and neglecting initial conditions, in the Laplace domain, via GHM method is (Park et al., 1998)

$$M_v s^2 x(s) + E^{\infty}\left(\sum_{n=1}^{k} \hat{a}_n \frac{s^2+2\hat{\varsigma}_m \hat{\omega}_n s}{s^2+2\hat{\varsigma}_n \hat{\omega}_n s+\hat{\omega}_n^2}\right) K_v(s)\, x(s) = F(s) \quad (13)$$

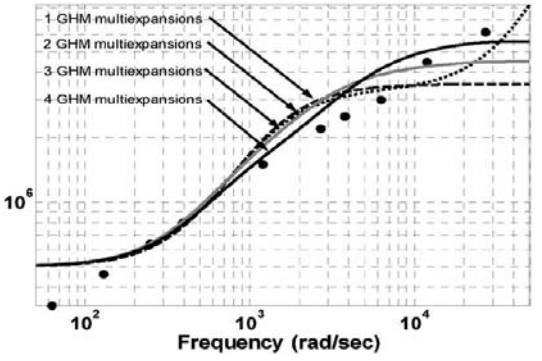

Fig. 5(a) Real part of GHM modulus function (∗ : true value, - : curve fitting)

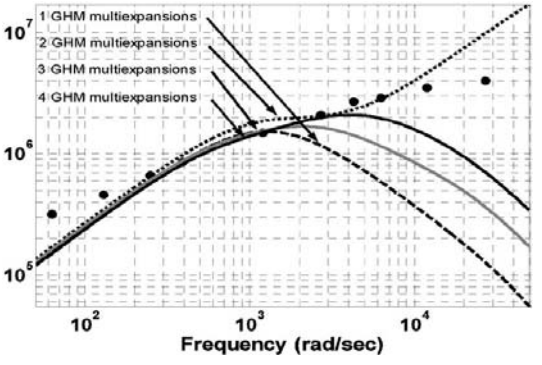

Fig. 5(b) Imaginary part of GHM modulus function (∗ : true value, - : curve fitting)

Such added degrees of freedom are also called internal variables. Eqs. (13) and (14) multiplied by E^{∞}, and the following equation of motion using the dissipation coordinate Eq. (14) can be assembled as

$$z(s) = \frac{\hat{\omega}^2}{s^2+2\hat{\varsigma}\hat{\omega}s+\hat{\omega}^2} x(s) \quad (14)$$

$$\begin{bmatrix} M_v & 0 \\ 0 & \dfrac{\hat{a}E^{\infty}}{\hat{w}}K_v \end{bmatrix}\begin{bmatrix} x(s) \\ z(s) \end{bmatrix} s^2 + \begin{bmatrix} 0 & 0 \\ 0 & \dfrac{2\hat{a}\hat{\varsigma}\varepsilon^{\infty}}{\hat{w}^2}K_v \end{bmatrix}\begin{bmatrix} x(s) \\ z(s) \end{bmatrix} s + \begin{bmatrix} (1+\hat{a})E^{\infty}K_v & -\hat{a}E^{\infty}K_v \\ -\hat{a}E^{\infty}K_v & \hat{a}E^{\infty}K_v \end{bmatrix}\begin{bmatrix} x(s) \\ z(s) \end{bmatrix} = \begin{bmatrix} F(s) \\ 0 \end{bmatrix} \quad (15)$$

where M_v and K_v are viscoelastic element mass and stiffness matrices, respectively.

4. Modeling Formulation of Composite-VEM Thin-Walled BEAM

Figure 6 represents the geometry and deformation of a beam composed of both composite material and viscoelastic material subjected to transversal loadings. The system configuration indicates a three layer sandwich beam in which the viscoelastic layer is sandwiched between constrained layer and base layer, which both are made of the same composite material. Herein, t_c, t_v and t_b denotes the thickness of constrained composite beam, viscoelastic beam and the base composite beam, respectively.

$$u_i(x,y,z,t) = u_{0,i} \quad (16)$$

$$v_i(x,y,z,t) = v_{0,i} \quad (17)$$

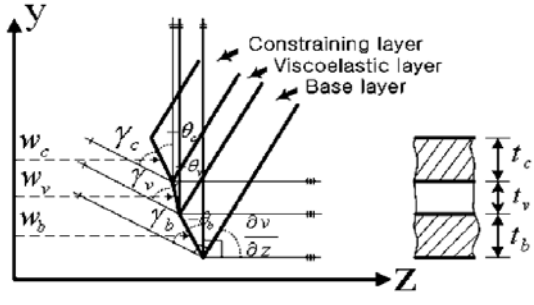

Fig. 6 Geometry of a beam including Composite-VEM-Composite layers during bending deformation

$$\theta_{x,i}(z,t)=\gamma_{yz,i}(z,t)-v_{0,i}'(z,t) \tag{18}$$

$$\theta_{y,i}(z,t)=\gamma_{xz,i}(z,t)+u_{0,i}'(z,t) \quad (i=b,v,c) \tag{19}$$

Eqs. (16)-(19) reveal that kinematic variables $u_0(z,t)$, $v_0(z,t)$, $\theta(z,t)$, $\theta_y(z,t)$ and representing two translations in the x, y directions and two rotations about the x, y directions, respectively are used to define the displacement components, u, and v in the present analysis. The transverse displacements u_i, $v_i(i=b,v,c)$ of all points on any cross section of the sandwich beam are considered to be constant in each flappingwise (v_i) and laggingwise (u_i) direction, respectively. The stiffness of composite material depends on the ply angle implemented in the thin-walled beam, the following relationships are needed to define shear strain in each layer (Ready, 1997; Hyer, 1997).

$$E_i=\frac{E_1}{m^4+\left(\frac{E_1}{G_{12}}-2\nu_{12}\right)n^2m^2+\frac{E_1}{E_2}n^4} \tag{20}$$

$$G_i=\frac{G_{12}}{n^4+m^4+2\left(2\frac{G_{12}}{E_1}(1+2\nu_{12})+2\frac{G_{12}}{E_2}-1\right)n^2m^2} \tag{21}$$

where $m=\cos\theta$, $n=\sin\theta$, $\theta=$ply angle are defined, respectively.

The shear strain in each layer is defined as Eq. (22) and corresponding magnitude is proportional to one another as indicated by Eq. (23):

$$\gamma_i=\frac{\tau}{G_i}=\frac{V}{G_ib(E_bI_b+E_vI_v+E_vI_v)}\int_A E_iydA \tag{22}$$

$$\gamma_b:\gamma_v:\gamma_c=P_b:P_v:P_c \tag{23}$$

Herein, P_b, P_v are P_c evaluated when the characteristic values of each layer are introduced in Eq. (22).

The following variables are introduced in the layer of VEM;

$$\theta_x^v=\frac{P_v}{P_b}\gamma_{yz,b}-y_{0,b}' \tag{24}$$

$$\theta_y^v=\frac{P_v}{P_b}\gamma_{xz,b}-u_{0,b}' \tag{25}$$

Furthermore, Eqs. (26) and (27) are introduced in the constrained layer;

$$\theta_x^c=\frac{P_c}{P_b}\gamma_{yz,b}-v_{0,b}' \tag{26}$$

$$\theta_y^c=\frac{P_c}{P_b}\gamma_{xz,b}-u_{0,b}' \tag{27}$$

5. Dynamic Equations of Rotating Contilevered Beams

Hamilton's variational principle is applied in order to obtain the equations of motion of adaptive rotating beams and the associated boundary conditions. The variational principle may be stated as

$$\delta J=\int_{t_0}^{t_1}\left[\int_\tau\sigma_{ij}\delta\varepsilon_{ij}d\tau-\delta K-\int_{\Omega_\sigma}\underline{s}_i\delta v_id\Omega-\int_\tau\rho H_i\delta v_id\tau\right]dt=0 \tag{28}$$

where

$$K=\frac{1}{2}\int_\tau\rho(\dot{\mathrm{R}}_i\cdot\dot{\mathrm{R}}_i)\,d\tau \tag{29}$$

In these equations, t_0 and t_1 denote two arbitrary instants of time; $d\tau(\equiv dnds dz)$ denotes the differential volume element, H_i denotes the components of the body forces; denotes the mass density; while δ denotes the variation operator. By using equations (1), (7)-(8), imposing Hamilton's conditions that $\delta v_i=0$ at t_0 and t_1, and performing the integration over the s and n directions, one obtains for the variation of kinetic energy and for the variation of the strain energy δV, respectively, (Oh et al., 2003), which are not displayed here.

These equations are represented in terms of 1-D stress resultants and stress couples. Within the present study, for the type of anisotropy considered herein, (i.e. CUS manufacturing technique) an exact split of the governing system of equations and of the associated BCs into two uncoupled subsystems arises. Since the analysis is confined here to rotating blades featuring coupled lagging and flapping motions only, the associated governing equations and boundary conditions for cantilevered beams are given explicitely as:

$$\delta u_0:(a_{44}(u_0'+\theta_y))'+(a_{43}\theta_x')'+\Omega^2[b_1R(z)u_0']'+b_1\Omega^2u_0-b_1\ddot{u}=0 \tag{30}$$

$$\delta v_0:(a_{55}(v_0'+\theta_x))'+(a_{52}\theta_y')+\Omega^2[b_1R(z)v_0']'-b_1\ddot{v}=P_m \tag{31}$$

$$\delta\theta_y:(a_{22}\theta_y')'+(a_{25}(v_0'+\theta_x))-a_{43}\theta_x' -a_{44}(u_0'+\theta_y)-(b_5+b_{15})(\ddot{\theta}_y-\Omega^2\theta_y)=0 \quad (32)$$

$$\delta\theta_x:(a_{33}\theta_x')'+(a_{34}(u_0'+\theta_y))'-a_{52}\theta_y' -a_{55}(v_0'+\theta_x)-(b_4+b_{14})(\ddot{\theta}_x-\Omega^2\theta_x)=0 \quad (33)$$

the Boundary Conditions: at $z=0$:

$$u_0=v_0=\theta_x=\theta_y=0 \quad (34a\text{-}d)$$

and at $z=L$:

$$\begin{aligned}\delta u_0&=a_{44}(u_0''+\theta_y')+a_{43}\theta_x''=0\\ \delta v_0&=a_{55}(v_0''+\theta_x')+a_{52}\theta_y''=0\\ \delta\theta_y&=a_{22}\theta_y''+a_{25}(v_0''+\theta_x')=0\\ \delta\theta_x&=a_{33}\theta_x''+a_{34}(u_0''+\theta_y')=0\end{aligned} \quad (35a\text{-}d)$$

Herein the coefficients a_{ij} and b_i denote stiffness, mass of composite structural properties, respectively, which were shown qualitatively in Shim and Na (2003).

6. Numerical Illustrations and Discussions

6.1 Model validation

The GHM methodology validation is achieved in the present part for the simple sandwich beam through the comparisons with numerical and experimental results found in the literature. The beam consisted of an aluminum base beam, with a layer of 3M ISD 112 viscoelastic material, followed by an aluminum constrained layer. It is assumed that the shear strains in the constrained layer and in the base beam are negligible. The transverse displacement of all points on any cross section of the sandwich beam are considered to be equal.

The material properties of base and constraining layer, and viscoelastic material used in simulation were given in Table 1. The first three eigenfrequencies and damping ratios are evaluated for a cantilevered sandwich beam with length 200 mm and width 10 mm. The 3M ISD112 viscoelastic material is modeled using GHM scheme, which parameters evaluated from a curve-fitting of the material master curves. One may notice that present results via GHM methodology based on assumed mode method match well with previous theoretical and numerical results in the literature without significant loss of accuracy.

Table 1 Characteristic values of sandwich beam

Paramete	Base Beam	VEM layer	Constrained layer
Young's Modulus (GN/m^2)	70	ISD 112	70
Mass density (kg/m^3)	2700	1600	2700
Thickness (mm)	5	0.25	1
Poisson's ratio	0.33	0.4	0.33

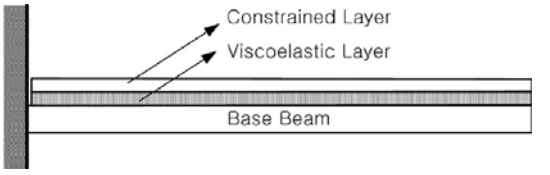

Fig. 7 Sandwiched beam with an Euler beam and a viscoelastic layer

After the methods outlined were tested on the cantilevered beam shown in Fig. 7, the GHM methodology is extended the composite thin-walled beam structure shown in Fig. 3.

The characteristic dimension values of a composite material and viscoelastic material were given in Table 2 and 3, respectively. Table 4 provides parametric values used in simulation of GHM methodology. For the free vibration problem, it is necessary to solve the closed-loop eigenvalue problem. To this end the unknown variables are represented in a generic form as

$$F(z,t)=\bar{F}(z)\exp(\lambda t) \quad (36)$$

Use of the representation (36) in Eqs. (30)-(33) associated with coupled flapping and lagging motion results in differential eigenvalue problems in terms of $\bar{u}_0(z)$, $\bar{\theta}_y(z)$, $\bar{v}_0(z)$ and $\bar{\theta}_x(z)$. The discretization of the obtained differential eigenvalue problem in the spatial domain was done via the extended Galerkin method which is carried out directly in the Hamilton's principle, Eq. (28). To this end $\bar{u}_0(z)$, $\bar{\theta}_y(z)$, $\bar{v}_0(z)$ and $\bar{\theta}_x(z)$ are expanded in series of trial functions satisfying the essential boundary condition. In the case of implementing viscoelastic material, the solution

of the algebraic eigenvalue problem yields the closed-loop eigenvalues

$$(\lambda_r, \overline{\lambda_r}) = \sigma_r \pm i\omega_{dr} \quad r = 1, 2, ..., n \qquad (37)$$

which σ_r is a measure of the damping in the r-th mode, while ω_{dr} is the r-th frequency of damped oscillations. The damping factor in the r-th mode results as

$$s_r = -\frac{\sigma_r}{(\sigma_r^2 + \omega_{dr}^2)^{1/2}} \qquad (38)$$

Table 5 shows the comparison of first three eigenfrequencies and damping ratios of composite structure between the Kelvin-Voigt method using measured complex modulus and the present GHM methodology.

Table 2 Characteristic Values of Graphite/Epoxy

Parameter	Value	Parameter	Value
L	2.032 m	G_{12}	3.103E9 N/m^2
$t_b = t_c$	0.00247 m	$G_{23} = G_{31}$	2.551E9 N/m^2
R	0.254 m	$\nu_{12} = \nu_{23} = \nu_{31}$	0.25
E_1	2.068E11 N/m^2	ρ	1528.28 Kg/m^3
$E_2 = E_3$	5.171E9 N/m^2		

Table 3 Characteristic Values of Viscoelastic Material (ISD-112)

Parameter	Value	Parameter	Value
L	2.032 m	G	5E5 N/m^2
t_v	2.477E-4m (5%)	ρ	1250 kg/m^3
E	1.4E6 N/m^2	ν	0.4

Table 4 Parametric Value of GHM

Parameter	Value
$\hat{a}$	6
$\hat{s}$	4
$\hat{w}$	10,000

6.2 The effects of VEM thickness on dynamic response of sandwich thin-walled structure

Figure 8 displays the loss factors of composite sandwich thin-walled structure with different ply

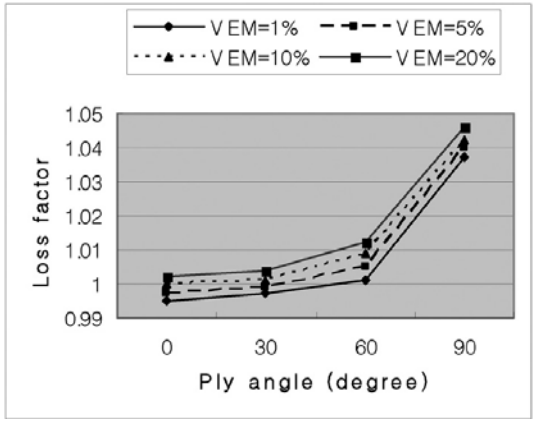

Fig. 8 Loss factors of structure with different ply angles for selected VEM thicknesses

Table 5 Natural frequencies and damping ratios of composite structures using 1-4 mini oscillators

ISD-112		Kelvin-Voigt[8]	1 mini oscillator[5]	2 mini oscillators	3 mini oscillators	4 mini oscillators
1 mode	Freq. (rad/s)	160	160	160	160	160
	Damping ratio (%)	0.820	0.620	0.700	0.660	0.619
2 mode	Freq. (rad/s)	226	227	227	227	227
	Damping ratio (%)	1.85	1.96	2.22	2.07	1.94
3 mode	Freq. (rad/s)	597	601	601	602	601
	Damping ratio (%)	2.98	3.77	4.32	3.68	3.45

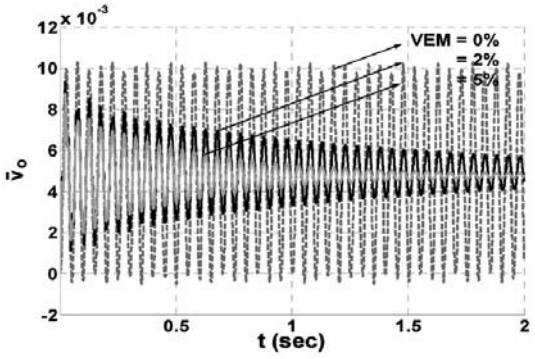

Fig. 9 Non-dimensional transversal deflections of the blade tip subjected to step loading for various VEM thicknesses (Ω=100 rad/s, θ=45°)

angles for a few selected VEM thicknesses. It can be seen from this figure that by increasing the thickness of the viscoelastic material and ply angles, higher damping can be obtained in the structure.

Also shown in Fig. 9 are nondimensional trasversal deflections as functions of time exposed to step loading as external exciations for various VEM thicknesses. The blade is rotating with 100 rad/s and ply angle is θ=45°. As expected from Fig. 9, the dynamic response amplitude of blade tip displacement is reduced as VEM thickness increases. However, it should be noticed that damping increase is not always a linear function of VEM thickness.

6.3 The effect of rotating speed to the dynamic response of thin-walled blade

Figure 10(a) and (b) depict the nondimensional flapping and lagging dynamic response of the blade rotating with three different speeds (Ω= 100, 200, 300 rad/s) for 5% of VEM thickness and θ=45°. The results reveal that an increase in rotational speed is accompanied by a decrease in response in both flapping and lagging direction, thus displaying centrifugal stiffening. A general remark emerging from Figs. 10 are that the stiffening effect due to beam rotation also contributes to the increase of natural frequencies.

6.4 The effect of ply angles to dynamic response of blade

Figure 11 obtained for the case of step loading

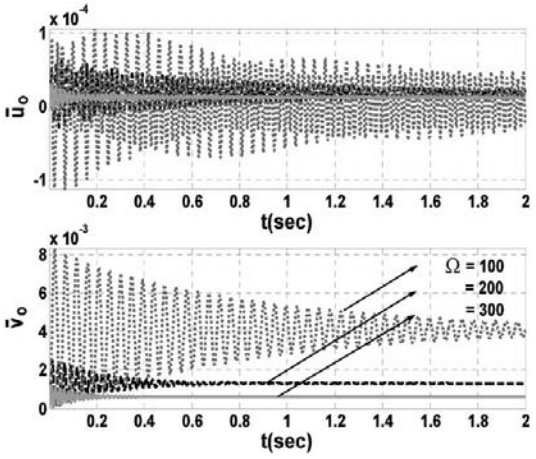

Fig. 10 (a), (b) Non-dimensional dynamic response of blade subjected to step loading with different rotating speeds

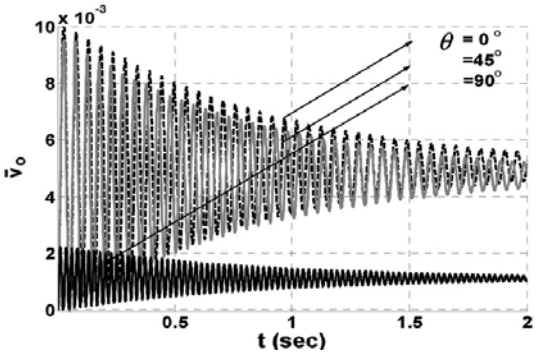

Fig. 11 Non-dimensional dynamic response of blade subjected to step loading with different ply angles

reveal an attenuation of dynamic response when using a larger ply angle, which implies increased flexural stiffness for larger ply angles. Hence, this directional property of fiber reinforced composites can be used for effective control via structural tailoring of the host structure together with viscoelastic material.

7. Conclusions

A dynamic structural model of rotating composite thin-walled beam of biconvex cross-sections including viscoelastic material was developed, and the effect of the inclusion of viscoelastic

material was assessed.

The dual technology including structural tailoring and passive damping technology is implemented in order to enhance the vibrational characteristics of the blade. Whereas structural tailoring methodology uses the directionality properties of advanced composite materials, the passive materials technology exploits the damping capabilities of viscoelastic material (VEM) embedded into the host structure. The VEM layer damping treatment is modeled by using the Golla-Hughes-McTavish(GHM) method. The case of VEM spread over the entire span of the structure is considered. The displayed numerical results provide a comprehensive picture of the synergistic implications of the application of both techniques, namely, the tailoring and damping technology on dynamic response of rotating thin-walled beam exposed to external time-dependent excitations. The obtained results reveal that via this control capability it is possible to tune conveniently the eigenfrequencies of the system, and consequently to modify in a beneficial and predictable way the dynamic response characteristics of the structure. It is also believed that this control capability can play a major role in enhancing the fatigue life of the structural booms for space missions, helicopter rotor blade as well as of tilt rotor aircraft.

References

DiTaranto R. A., 1965, "Theory of Vibratory Bending for Elastic and Viscoelastic Layered Finite-Length Beams," *ASME Journal of Applied Mechanics*, Vol. 32, pp. 881～886.

Hyer, M. W., 1997, "Stress Analysis of Fiber-Reinforced Composote Materials," WCB McGraw-Hill.

Kerwin, E. M., 1959, "Damping of Flexural Waves by a Constrained Viscoelastic Layer," *Journal of the Acoustical Society of America*, Vol. 31 pp. 952～962.

Lam, M. J., Inman, D. J. and Saunders, W. R., 1997, "Vibration Control through Passive Constrained Layer Damping and Active Control," *Journal of Intelligent Material System and Structures*, Vol. 8, pp. 663～677.

McTavish, D. J. and Hughes, P. C., 1992, "Finite Element Modeling of Linear Viscoelastic Structures : the GHM Method," AIAA-92-2380, pp. 1753～1763.

Mead, D. J. and Markus, S., 1969, "The Force Vibration of a Three Layer Damped Sandwich Beam with Arbitrary Boundary Conditions," *Journal of Sound and Vibration*, Vol. 10, pp. 163～175.

Oh, S., Song, O. and Librescu, L., 2003, "Effect of Pretwist and Presetting on Coupled Bending Vibrations of Rotating Thin-walled Composite Beams," *International Journal of Solids and Structures* 40, pp. 1203～1224.

Park, C. H., Ahn, S. J., Park, H. and Na, S., 2005, "Modeling of a Hybrid Passive Damping System," *Journal of Mechanical Science and Technology*, 19(1), pp. 127～135.

Park, C., Kim, W. and Yang, B.,1998, "Vibration Analysis of Three Layer Sandwich Beam," *Journal of KSNVE*, Vol. 8, pp. 157～170.

Rao, YVKS and Nakra, B. C., 1974, "Vibrations of Unsymmetrical Sandwich Beams and Plates with Viscoelastic Cores," *Journal of Sound and Vibration*, Vol. 34, pp. 309～326.

Ready, J. N., 1997, *Mechanics of Laminated Composite Plates*, Theory and Analysis, CRC Press.

Ross, D., Ungar, E. and Kerwin, E., 1959, "Flexural Vibrations by Means of Viscoelastic Laminate," *ASME Structure Damping*, pp. 48～87.

Shim, J. K. and Na, S. S., 2003, "Modeling and Vibration Feedback Control of Rotating Tapered Composite Thin-Walled Blade," *KSME International Journal*, Vol. 17, No. 3, pp. 380～390.